Photon-pair generation by four-wave mixing in optical fibers

Q. Lin, F. Yaman, and Govind P. Agrawal

Institute of Optics, University of Rochester, Rochester, New York 14627

Received October 4, 2005; revised December 20, 2005; accepted January 12, 2006; posted February 6, 2006 (Doc. ID 65168)

We present a theory to quantify a fundamental limit on correlated photon pairs generated through four-wave mixing inside optical fibers in the presence of spontaneous Raman scattering (SpRS). Our theory is able to explain current experimental data. We show that if correlated photon pairs are generated with polarization orthogonal to the pump the effect of SpRS is significantly reduced over a broad spectral region extending from 5 to 15 THz. © 2006 Optical Society of America

OCIS codes: 190.4380, 190.5650, 060.4370, 270.0270, 270.5290.

Entangled photon pairs are essential for applications related to quantum information processing. Four-wave mixing (FWM) in optical fibers can generate correlated photon pairs with high brightness.[1,2] However, recent experiments show[3–8] that this scheme is severely deteriorated by spontaneous Raman scattering (SpRS), which contributes significantly to accidental coincidence counting and limits the available frequency range of correlated photon pairs. With a complete neglect of the Raman response,[9] current theories[1,2] cannot describe such an effect of SpRS, and empirical fitting is widely used in practice.[3–8] As FWM becomes promising for fiber-based photon sources, it is important to develop an appropriate theory for guiding practical photon-pair generation.[7] In this Letter, we present such a theory.

In the Heisenberg picture, the two polarization components of the field operator, $\hat{A}_i(z,\tau)$ $(i=x,y)$, satisfy[10,11]

$$\frac{\partial \hat{A}_i}{\partial z} = i\sum_j \int_{-\infty}^{\tau} d\tau' R_{ij}^{(1)}(\tau-\tau')\hat{A}_j(z,\tau') + i\sum_j \hat{m}_{ij}(z,\tau)\hat{A}_j(z,\tau) + i\sum_{jkl}\int_{-\infty}^{\tau} d\tau' R_{ijkl}^{(3)}(\tau-\tau')\hat{A}_k^{\dagger}(z,\tau')\hat{A}_l(z,\tau')\hat{A}_j(z,\tau), \quad (1)$$

where $R_{ij}^{(1)}$ describes the linear dispersive properties, including birefringence, and $R_{ijkl}^{(3)}$ is the third-order nonlinear response for silica fibers given by[12]

$$R_{ijkl}^{(3)}(\tau) = \frac{\gamma}{3}(1-f_R)\delta(\tau)(\delta_{ij}\delta_{kl}+\delta_{ik}\delta_{jl}+\delta_{il}\delta_{jk}) + \gamma f_R R_a(\tau)\delta_{ij}\delta_{kl} + \frac{\gamma}{2}f_R R_b(\tau)(\delta_{ik}\delta_{jl}+\delta_{il}\delta_{jk}), \quad (2)$$

where $R_a(\tau)$ and $R_b(\tau)$ are the isotropic and anisotropic Raman responses and f_R represents their fractional contribution to the nonlinear refractive index. $\hat{m}_{ij}$ is the noise operator (related to the phonon reservoir), and nonlinear parameter $\gamma=n_2\omega_p/ca_{\text{eff}}$, where a_{eff} is the effective core area.

We focus on the degenerate FWM induced by a single pump wave launched at ω_p. Photon energy conservation requires $2\omega_p=\omega_s+\omega_i$, where ω_s and ω_i are the frequencies of the signal and idler photons, respectively. In most experiments, pump pulses are wide enough in time that the dispersion length is much longer than the fiber length. As a result, the pump can be assumed to be quasi-continuous. Moreover, as the pump is much more intense than the signal and the idler, it can be treated classically and assumed to remain undepleted. We also assume that the pump wave is linearly polarized along a principal axis of the fiber, say, the x axis. It is easy to show that the Kerr nonlinearity imposes only a phase modulation on the pump wave, which evolves as $A_{px}(z)=A_p\Phi(z)$, where the phase factor $\Phi(z)=\exp\{i[k_x(\omega_p)+\gamma P_0]z\}$, $P_0=|A_p|^2$ is the pump power and $k_x(\omega_p)$ is the propagation constant.

It turns out that the FWM process can be decoupled into two independent "eigenprocesses," shown in Fig. 1. Decomposing Eq. (1) in the spectral domain, we obtain the Heisenberg equations for the two polarizations of the signal as

$$\frac{\partial \hat{A}_j(z,\omega_s)}{\partial z} = i[k_j(\omega_s)+\gamma\xi_j(\Omega_s)P_0]\hat{A}_j(z,\omega_s) + i\gamma\eta_j(\Omega_s)A_{px}^2\hat{A}_j^{\dagger}(z,\omega_i) + iA_{px}\hat{m}_{jx}(z,\Omega_s), \quad (3)$$

where $j=x,y$, k_j is the propagation constant, and $\Omega_s=\omega_s-\omega_p$. The idler equation can be obtained by exchanging the subscripts s and i. The signal and idler fields are normalized to satisfy $[\hat{A}_j(z,\omega_\mu),\hat{A}_k^{\dagger}(z,\omega_\nu)]=2\pi\delta_{jk}\delta(\omega_\mu-\omega_\nu)$.

The complex quantities $\xi_x=2-f_R+f_R\tilde{R}_a(\Omega_s)+f_R\tilde{R}_b(\Omega_s)$ and $\xi_y=2(1-f_R)/3+f_R\tilde{R}_a(0)+f_R\tilde{R}_b(\Omega_s)/2$, where a tilde denotes a Fourier transform, include both cross-phase modulation and Raman scattering as the imaginary parts of $\tilde{R}_a$ and $\tilde{R}_b$ provide the co-

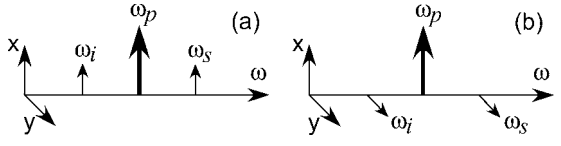

Fig. 1. Two eigenprocesses of FWM. The signal and idler are copolarized with the pump during process (a) but are orthogonally polarized during process (b).

0146-9592/06/091286-3/$15.00

polarized and orthogonally polarized Raman gain/loss as[12] $g_{Rx}(\Omega_s) \equiv 2\gamma f_R \,\mathrm{Im}[\tilde{R}_a(\Omega_s)+\tilde{R}_b(\Omega_s)]$ and $g_{Ry}(\Omega_s) \equiv \gamma f_R \,\mathrm{Im}[\tilde{R}_b(\Omega_s)]$, respectively. Coupling to the phonon mode at frequency $|\Omega_s|$ introduces SpRS that is represented by the operator $\hat{m}_{jx}(z,\Omega_s)$. It satisfies the commutation relation[10,11] of $[\hat{m}_{jx}(z_1,\Omega_\mu),\hat{m}^\dagger_{jx}(z_2,\Omega_\nu)] = 2\pi g_{Rj}(\Omega_\mu)\delta(\Omega_\mu-\Omega_\nu)\delta(z_1-z_2)$.

FWM efficiency is related to η_j that is different for the two eigenprocesses: $\eta_x = 1-f_R+f_R\tilde{R}_a(\Omega_s) + f_R\tilde{R}_b(\Omega_s)$ and $\eta_y = (1-f_R)/3 + f_R\tilde{R}_b(\Omega_s)/2$. In practice, the first term dominates, and copolarized FWM is roughly three times more efficient than the orthogonally polarized FWM. For this reason, most recent experiments[3–8] have focused on the copolarized configuration. However, this approach has a serious drawback because SpRS is also maximized when the pump and the signal/idler are copolarized. Moreover, the Raman response also changes the refractive index through the Kramers–Kronig relation and thus affects the FWM efficiency.[9] The magnitude of η_x decreases by ~20% when the signal is detuned far beyond the Raman gain peak.

Equation (3) can be solved to yield the following solution for the signal wave for a fiber of length L:

$$\hat{A}_j(L,\omega_s) = [\alpha_j(L,\omega_s)\hat{A}_j(0,\omega_s) + \beta_j(L,\omega_s)\hat{A}_j^\dagger(0,\omega_i) + \hat{N}_j(L,\omega_s)]\Phi(L), \quad (4)$$

where the coefficients are given by

$$\alpha_j(L,\omega_s) = [\cosh(g_jL) + (i\kappa_j/2g_j)\sinh(g_jL)]e^{iK_jL}, \quad (5)$$

$$\beta_j(L,\omega_s) = (i\gamma\eta_j/g_j)A_p^2\sinh(g_jL)e^{iK_jL}, \quad (6)$$

$$\hat{N}_j(L,\omega_s) = i\int_0^L \hat{m}_{jx}(z,\Omega_s)[A_p\alpha_j(L-z,\omega_s) - A_p^*\beta_j(L-z,\omega_s)]\mathrm{d}z, \quad (7)$$

where g_j is the parametric gain coefficient given by $g_j^2 = (\gamma\eta_jP_0)^2 - (\kappa_j/2)^2$, $\kappa_j = k_j(\omega_s)+k_j(\omega_i)-2k_x(\omega_p) + 2\gamma P_0(\xi_j-1)$ represents the phase mismatch, and $K_j = [k_j(\omega_s)-k_j(\omega_i)]/2$.

In general, the two FWM processes in Fig. 1 have different phase-matching conditions because of the fiber birefringence, and only one of them is used in a given experiment for photon generation. As the two processes have the same form of solution as Eq. (4), we can drop the polarization subscript $j=x,y$, provided that appropriate ξ, η, κ, and g are used. In practice, the signal and idler fields are filtered to limit their bandwidth as $\hat{A}_\mu(\tau) = \int H_\mu(\omega-\omega'_\mu)\hat{A}(L,\omega)\exp(-i\omega\tau)\mathrm{d}\omega/2\pi$, where $H_\mu(\omega-\omega'_\mu)$ is the filter transmission function centered at ω'_μ ($\mu=s,i$). Filters are positioned at the center of the phase-matched window, where $\mathrm{Re}(\kappa)\approx 0$, and selected such that $\omega'_s+\omega'_i = 2\omega_p$, where we denote the signal as the anti-Stokes with $\omega'_s > \omega_p$.

For photon-pair generation, the pump power is kept low enough that $\gamma P_0 L \ll 1$ to prevent stimulated scattering. Using Eqs. (4)–(7), we find that the photon flux, $I_\mu \equiv \langle\hat{A}^\dagger_\mu(\tau)\hat{A}_\mu(\tau)\rangle$ in this low power regime is given by $I_\mu = \Delta\nu_\mu(|\gamma P_0\eta L|^2 + P_0L|g_R|\mathcal{N}_\mu)$, where $\mu=s,i$, $\mathcal{N}_s = n_{\mathrm{th}}$ but $\mathcal{N}_i = n_{\mathrm{th}}+1$, and $n_{\mathrm{th}} = [\exp(\hbar|\Omega_0|/k_BT)-1]^{-1}$ is the phonon population at frequency $\Omega_0 = \omega'_s-\omega_p$ and at temperature T. $\eta = \eta(\Omega_0)$, $g_R = g_R(\Omega_0)$, and filter bandwidth $\Delta\nu_\mu$ is defined as $\Delta\nu_\mu = \int|H_\mu(\omega-\omega'_\mu)|^2\mathrm{d}\omega/2\pi$. As expected, the photon flux consists of two sources: one is FWM that grows quadratically with both pump power and fiber length, and the other is SpRS that grows linearly and generates more idler photons than signal photons. Clearly, $\gamma P_0 L$ should be maintained at an appropriately low level, large enough to make FWM dominate but small enough to prevent stimulated scattering. As a result, SpRS remains as a dominant degradation source.

The quantum correlation between signal and idler photons can be well quantified by the ratio between true and accidental coincidence, defined as

$$\rho(\tau) = \langle\hat{A}_i^\dagger(t)\hat{A}_s^\dagger(t+\tau)\hat{A}_s(t+\tau)\hat{A}_i(t)\rangle/(I_sI_i) - 1, \quad (8)$$

where $\langle\hat{A}_i^\dagger(t)\hat{A}_s^\dagger(t+\tau)\hat{A}_s(t+\tau)\hat{A}_i(t)\rangle$ is the biphoton probability of the signal–idler pair. Using Eqs. (4)–(7), we are able to obtain the following simple expression when $\gamma P_0 L \ll 1$:

$$\rho(\tau) = \frac{|\varphi(\tau)|^2\{[\gamma\,\mathrm{Re}(\eta)]^2 + |g_R(n_{\mathrm{th}}+1/2)|^2\}}{[|\gamma\eta|^2P_0L + |g_R|(n_{\mathrm{th}}+1)](|\gamma\eta|^2P_0L + |g_R|n_{\mathrm{th}})}, \quad (9)$$

where $\varphi(\tau)$ is related to the two filters as $\varphi(\tau) = (\Delta\nu_s\Delta\nu_i)^{-1/2}\int H_s(\omega-\omega'_s)H_i(\omega'_s-\omega)e^{-i\omega\tau}\mathrm{d}\omega/2\pi$. Clearly, the correlation decreases with increased pump power because of an increased probability of simultaneous multiphoton generation, as was observed experimentally.[4,6,7] SpRS contributes little to the true coincidence, but it introduces considerable accidental coincidence and thus reduces the correlation value. For a pure FWM process without SpRS, η is real and the correlation reduces to $\rho(\tau) = |\varphi(\tau)|^2/|\gamma\eta P_0 L|^2$.

Equation (9) constitutes our main result. In what follows, we use it to discuss some typical experimental results and to propose a new scheme. Figure 2 shows $\rho(0)$ as a function of pump–signal detuning for the two polarization configurations shown in Fig. 1, assuming identically shaped signal and idler filters such that $|\varphi(0)|^2 \approx 1$. In the orthogonal configuration we increase P_0 by a factor of 3 so that FWM creates nearly the same number of photons in the two cases.

When the signal is close to the pump (say, detuning of 0.5 THz), correlation is about 12 for a typical value of $\gamma P_0 L \approx 0.15$ but reduces to 3.5 when $\gamma P_0 L$ increases to 0.4, indicating that current experiments around this regime[3,4,6] are close to the fundamental limit. In the copolarized case (dotted curves), the correlation remains small over a broad range, 2–15 THz, reflecting the degrading effect of SpRS. However, the correlation increases to high values when the signal is detuned far beyond the Raman-gain peak (but with ~40% reduction in FWM-

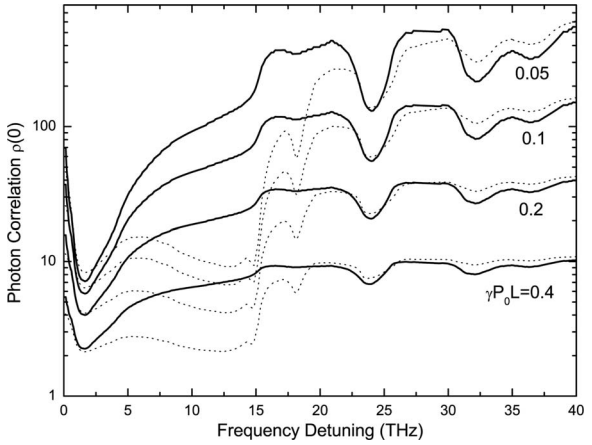

Fig. 2. Correlation $\rho(0)$ versus pump–signal detuning, assuming perfect phase matching, for $n_2=2.6\times10^{-20}$ m^2/W, peak Raman gain of 0.62×10^{-13} m/W (at 1550 nm), and $T=300$ K. The Raman spectra used are from Ref. 9. The dotted and solid curves show the copolarized and orthogonally polarized cases, respectively.

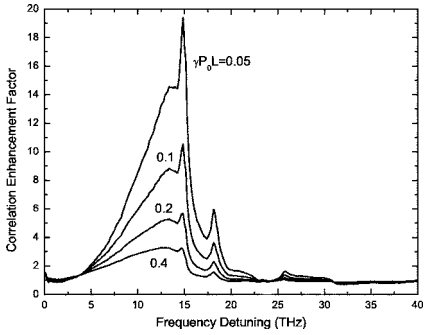

Fig. 3. Correlation enhancement factor plotted as a function of pump–signal detuning.

generated photons due to a Raman-induced decrease in FWM efficiency). For example, around 30 THz, the correlation varies from 138 to 39 for $\gamma P_0 L=0.1-0.2$ and can increase to 450 when $\gamma P_0 L$ is decreased to 0.05. For this reason, several experimental groups have made efforts to operate around this regime or even farther.[5,7,8] Consider the data of Ref. 7. With a pump–signal detuning of 28 THz near 735 nm, Eq. (9) shows that $\rho(0)$ is 2105, 42, and 17 for $\gamma P_0 L$ values of 0.0155, 0.19, and 0.31, respectively (corresponding to average powers of 0.05, 0.6, and 1 mW, respectively, in Ref. 7). These values are higher than the experimentally measured correlation of 300, 23, and 10 at these power levels, implying the possibility of further experimental improvement. A large discrepancy at the lowest pump level is likely due to dark counting, which tends to dominate accidental coincidence when the photon rate is low.

Figure 2 shows that high-quality photon pairs can be generated with copolarized FWM only far from the pump (by at least 20 THz). However, they can be obtained over a broad spectral region below 20 THz when the photon pairs are generated with polarization orthogonal to the pump (solid curves). The Raman gain is almost negligible in this configuration,[9] a feature that improves the correlation $\rho(0)$ considerably. The most improvement occurs in the detuning range of 5 to 15 THz, the same range where the copolarized configuration is the worst. Near the copolarized Raman-gain peak close to 13 THz, correlation can be increased from a value of 4–7 to more than 20–60 for $\gamma P_0 L=0.1-0.2$.

We quantify the increase in the correlation for the orthogonally polarized case by a figure of merit defined as the ratio of $\rho(0)$ in the orthogonal and copolarized cases at a given detuning, as shown in Fig. 3. Clearly, orthogonally polarized FWM exhibits correlation enhancement over a broad spectral range. When the power level is low, photon generation is dominated by SpRS in the copolarized case but is dominated by FWM in the orthogonally polarized case, resulting in a significant correlation enhancement of close to 20 for $\gamma P_0 L=0.05$. The enhancement factor decreases with increased power level because FWM tends to dominate at high power levels. For $\gamma P_0 L=0.1-0.2$, the enhancement factor is 5–10 over a broad spectral region around the Raman gain peak.

We have presented a vector theory to quantify photon-pair generation inside optical fibers and used it to explain the current experimental results. We suggest a new configuration in which photon pairs are generated with polarization orthogonal to the pump and show that it significantly reduces the effect of SpRS over a broad spectral region where the copolarized FWM suffers from severe SpRS. In practice, such orthogonally polarized FWM can be realized in low-birefringence fibers.[13] Note that a fiber with random birefringence can be used only if its length is shorter than the birefringence correlation length.

This work was supported by National Science Foundation grants ECS-0320816 and ECS-0334982.

References

1. L. J. Wang, C. K. Hong, and S. R. Friberg, J. Opt. B Quantum Semiclassical Opt.**3**, 346 (2001).
2. J. Chen, X. Li, and P. Kumar, Semiclassical Opt. **72**, 033801 (2005).
3. X. Li, J. Chen, P. Voss, J. Sharping, and P. Kumar, Opt. Express **12**, 3737 (2004).
4. K. Inoue and K. Shimizu, Jpn. J. Appl. Phys. Part 1 **43**, 8048 (2004).
5. J. G. Rarity, J. Fulconis, J. Duligall, W. J. Wadsworth, and P. St. J. Russell, Opt. Express **13**, 534 (2005).
6. J. Fan, A. Dogariu, and L. J. Wang, Opt. Lett. **30**, 1530 (2005).
7. J. Fan, A. Migdall, and L. J. Wang, Opt. Lett. **30**, 3368 (2005).
8. J. Fulconis, O. Alibart, W. J. Wadsworth, P. St. J. Russell, and J. G. Rarity, Opt. Express **13**, 7572 (2005).
9. R. H. Stolen, in *Raman Amplifiers for Telecommunications 1*, M. N. Islam, ed. (Springer, 2003). The Raman spectra are provided by R. H. Stolen.
10. P. D. Drummond, in *Coherence and Quantum Optics VII*, J. H. Eberly, L. Mandel, and E. Wolf, eds. (Springer, 1996), p. 323.
11. L. Boivin, F. X. Kärtner, and H. A. Haus, Phys. Rev. Lett. **73**, 240 (1994).
12. R. W. Hellwarth, Prog. Quantum Electron. **5**, 1 (1977).
13. S. G. Murdoch, R. Leonhardt, and J. D. Harvey, Opt. Lett. **20**, 866 (1995).